PHYSICAL REVIEW B **73**, 045407 (2006)

Temperature dependent normal and anomalous electron diffusion in porous TiO_2 studied by transient surface photovoltage

Thomas Dittrich
Hahn-Meitner-Institut, Glienicker Str. 100, D-14109 Berlin, Germany

Iván Mora-Seró, Germà García-Belmonte, and Juan Bisquert
Departament de Ciències Experimentals, Universitat Jaume I, 12071 Castello, Spain
(Received 21 September 2005; revised manuscript received 19 October 2005; published 11 January 2006)

A model system of nanoporous TiO_2 sensitized with dye molecules at the outer surface is investigated by time resolved surface photovoltage (SPV) at temperatures between −120 °C and 270 °C to get information about electron diffusion over more than 10 orders of magnitude in time. The SPV transients increase in time due to independent electron diffusion and reach a maximum at a certain peak time due to reaching the screening length. The increasing parts of the SPV transients are characterized by a power law while the SPV power coefficient amounts to half of the dispersion parameter of anomalous diffusion. Anomalous diffusion is observed for times down to the duration time of the laser pulse (150 ps). With increasing temperature, the SPV power coefficient increases to its saturation value of 0.5 corresponding to normal diffusion. At lower temperatures, the SPV power coefficients decrease with increasing intensity of the exciting laser pulses. The decay of the SPV transients is determined by thermally activated normal diffusion. The minimal charge transfer time of an electron back to the positively charged dye molecule amounts to 2 ps which is obtained from thermally activated logarithmic decays.

DOI: 10.1103/PhysRevB.73.045407 PACS number(s): 72.40.+w, 73.63.Bd

INTRODUCTION

Spatial charge separation as well as electron diffusion play a crucial role in many biological, chemical, and physical systems. Charge separation takes place at very different time and length scales depending on the investigated system. For example, charge separation may proceed within tens of fs during ultrafast injection from dye molecules into TiO_2 (Ref. 1) or over long times during diffusion in a porous semiconductor.[2] In devices such as nanostructured solar cells,[3,4] it is important to clarify the time and length scales at which the related processes of initial charge separation, electron diffusion, and recombination take place, especially considering the strong energy disorder that affects both the diffusion and recombination of electrons[5] in these structures. It is recognized that the dynamics of electrons photoinjected from dye molecules into nanoscale semiconductor networks is composed of a hierarchy of processes spanning many orders of magnitude in time. Normal and anomalous diffusion belong to these processes.

Techniques operating in the low frequency range (10 mHz–1000 Hz) such as impedance spectroscopy or itensity-modulated photocurrent spectroscopy[6] provide macroscopic parameters that are time and spatial averaged with respect to the microscopic processes. The latter are resolved separately in fast optical pump-probe experiments (10 ns–10 ms), for example, monitoring the decay of the photoinduced dye cation excited by a laser pulse.[5] However, direct information about the spatial separation of carriers cannot be obtained from an optical measurement itself. In contrast, the surface photovoltage (SPV) technique[7] is a locally sensitive technique and it can be used to study the spatial charge separation induced by diffusion even over very short distances of the order of a nm.

In previous work, we showed that independent diffusion of excess charge carriers plays a dominant role for the formation of strongly retarded SPV transients in nanoporous TiO_2.[2] However, a detailed analysis of electron diffusion is rather difficult in these experiments since both excess electrons and holes were generated in the TiO_2 nanoparticles. In this work, we use a model system of nanoporous TiO_2 sensitized with dye molecules at the outer surface (see Fig. 1). Excess electrons are injected from excited dye molecules into TiO_2 nanoparticles. By this way, light induced positive charge remains fixed at the surface and electron diffusion can be investigated in more detail.

In the first part of this work, we give some theoretical considerations demonstrating the influence of normal diffu-

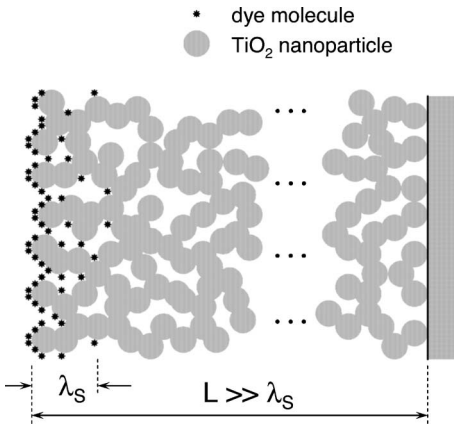

FIG. 1. Sketch of the investigated structure consisting of an interconnected network of TiO_2 nanoparticles dyed in the outer surface region. The screening length of the system is much shorter than the sample thickness.

sion, dielectric relaxation, screening length, and anomalous diffusion on SPV transients. It will be shown that the peak time of the SPV transients is proportional to the dielectric relaxation time and that the SPV transients follow a power law with a power coefficient half of the power coefficient of anomalous diffusion. In the second part, details about the experiments are given. Experimental results will be shown for the temperature and intensity dependent logarithmic decay time and power coefficients in the third part. We will demonstrate on dye sensitized nanoporous TiO_2 that the SPV bears the opportunity to get information about electron diffusion even at time scales down to the ps range. A change from anomalous to normal diffusion has been observed at short times when the SPV signal increases and at long times when the SPV signal decays, respectively. This behavior and the relation of the power coefficients to a distribution of states will be discussed in the fourth part of this work.

THEORETICAL CONSIDERATIONS FOR DIFFUSION SPV

The SPV measured in the investigated nanoporous TiO_2 is determined by the distribution of the electrons that were injected from the dye molecules absorbed at the outer surface of the porous TiO_2 layer (Fig. 1). Although there are no mobile holes in this system, it is important to take into account the presence of additional shielding charges in the bulk of the porous electrode,[8] which may screen the electrical field formed by the diffusing electrons. Shielding affects the SPV both in a temporal scale, the dielectric relaxation time, and in a spatial scale, the screening length λ_S. In a homogeneous medium, λ_S would be the Debye screening length (λ_D)

$$\lambda_S \approx \lambda_D = \sqrt{\frac{\varepsilon\varepsilon_0 kT}{ne^2}}, \tag{1}$$

where e is the elementary charge, $\varepsilon_0 = 8.85 \times 10^{-14}$ F/cm, ε is the dielectric constant, n is the concentration of free charge carriers, k is the Boltzmann constant and T is the temperature. Therefore the investigated system has two length scales, the layer thickness (L) and the screening length (λ_S) while $L \gg \lambda_S$. Electrons being separated by distances longer than the λ_S do not contribute anymore to the photovoltage since they are screened in the bulk. Therefore, the SPV signal is sensitive to charge separation between the initial charge separation length and λ_S. Values of λ_S are usually of the order of tens of nm in porous TiO_2 (Ref. 8) and SPV transients are independent of the layer thickness, for example, in the case of porous TiO_2 layers.[9]

In the following we will analyze the SPV of diffusing electrons with two different models. In the first one the diffusion phototovoltage is limited by a homogeneous shielding process described by a relaxation time and in the second one the SPV is limited to the screening length in the region close to the outer surface. Clearly, the two models are closely related and could be joined in a single model containing both the temporal and spatial details of electrical field screening. However, developing such model is complicated by the complex morphology and the lack of information on the dynamics and distribution of the shielding charges. Therefore both effects will be separately analyzed. It will be seen that both models predict an increase of the SPV for low times with a slope 1/2 in log-log scale, and the apparition of a peak in the SPV spectra at a time proportional to the dielectric relaxation time. But the behavior after this peak is attained differs in the two models, being the second model the one that allows to explain better the experimental results. Additionally we will also show the influence of the anomalous diffusion in the slope of the incrementing SPV for low times.

Diffusion photovoltage limited to relaxation time

Let us assume that the decay of the SPV is determined by the dielectric relaxation of the electrons in their own electrical field and the diffusion equation of the electron concentration is given by[10]

$$\frac{\partial}{\partial t}n(x,t) = D\frac{\partial^2}{\partial x^2}n(x,t) + \frac{n(x,t)-n_0}{\tau_M}, \tag{2}$$

where D, n_0, and τ_M are the diffusion coefficient, equilibrium electron concentration, and dielectric relaxation time ($\tau_M = \varepsilon\varepsilon_0/e\mu n$, μ is the mobility), respectively. Excess electrons $\Delta n = n - n_0$ are injected at the outer boundary of the film forming a semi-Gaussian with standard deviation $\sigma^2 = 2Dt_0$, where t_0 is a constant that characterizes the initial distribution. Equation (2) is solved numerically with reflecting boundary conditions. The injected electrons first diffuse away from the injecting contact and then decay homogeneously.

The SPV transient is calculated from the double integration of the Poisson equation of the time-dependent distribution of the excess electrons:

$$\mathrm{SPV} = U(t) = \frac{e}{\varepsilon\varepsilon_0}\int_0^d dx \int_0^x \Delta n(y,t)dy. \tag{3}$$

The calculated SPV transients shown in Fig. 2 record the different stages of the dynamic evolution. It starts at nonzero value (t_0) related to the initial charge separation, then increases as the carriers depart from the boundary and increase the separation length, and finally decreases due to disappearance of excess carriers. In the rising regime, the total number of carriers is constant (at times $t \ll \tau_M$) and the increase of PV is related only to the increase of the distance between negative and positive excess charge. Shifting the origin of time to t_0 and taking into account the diffusion law, $r^2 \propto Dt$, it is obtained the dependence $U \propto \sigma \propto (t+t_0)^{1/2}$ at the increasing part of the SPV transients. The decay regime corresponding to the linear relaxation process in Eq. (2) is a simple exponential and leads to the formation of a peak time (t_{peak}). The value of t_{peak} is proportional to τ_M with a proportionality factor of 2.7 as shown in the inset of Fig. 2. This example shows that SPV technique has the ability to distinguish clearly diffusion and recombination regimes even in very short time scales which are beyond the capabilities of the low frequency techniques.

Diffusion photovoltage limited to the screening length

Usually, SPV transients decay much slower than with a certain relaxation time due to limitation by diffusion or

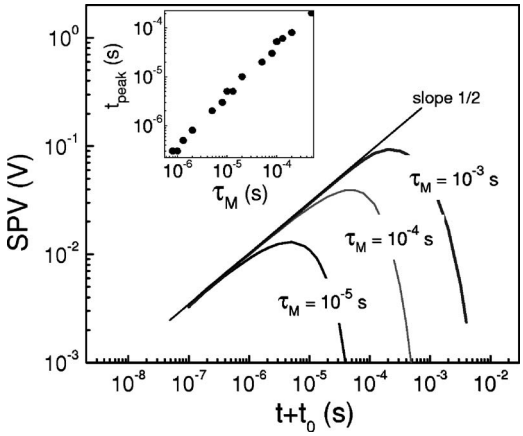

FIG. 2. SPV transients obtained by integration of the carrier distribution calculated by the simple diffusion model with three relaxation times (diffusion coefficient $D=10^{-3}$ cm^2 s^{-1}). The injected distribution at $t=0$, $x=0$, is a semi-Gaussian with equivalent time parameter $t_0=\sigma^2/D=10^{-7}$ s. The inset shows the correlation between the peak time of the SPV transients and the dielectric relaxation time.

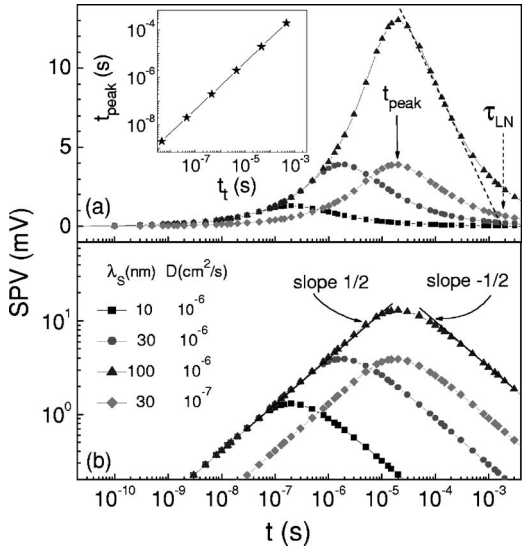

FIG. 3. SPV transients [(a) lin-log scale; (b) log-log scale] obtained by Eq. (5) which takes into account a boundary for integration given by λ_S (10, 30, 100 nm). The diffusion coefficients were 10^{-6} and 10^{-7} cm^2/s. The inset gives the dependence of t_{peak} on the time t_t given by Eq. (6). The definition of the logarithmic decay time is given as well.

tunneling.[11] For very thin layers, i.e., $L<\lambda_S$, both diffusion and double integration of the Poisson equation are given by the layer thickness.[11] For thick layers when $L\gg\lambda_S$, the double integration of the Poisson equation is restricted to the near surface region with the thickness λ_S. The solution of the diffusion equation

$$\frac{\partial}{\partial t}n(x,t)=D\frac{\partial^2}{\partial x^2}n(x,t) \tag{4}$$

is a semi-Gaussian in the case of a semi-infinite half-space and blocking boundary condition at $x=0$ (see Appendix A). The analytical solution of Eq. (4) is

$$\text{SPV}(t)=\frac{2en_i}{\sqrt{\pi}\varepsilon\varepsilon_0}\sqrt{Dt}\left[1-\exp\left(-\frac{\lambda_S^2}{4Dt}\right)\right]. \tag{5}$$

The value of n_i is the concentration of injected charge normalized to the area. The width of the semi-Gaussian is $\sigma=\sqrt{2Dt}$. It is reasonable to determine a transit time at which $\sigma(t)=\lambda_S$,

$$t_t=\frac{\lambda_S^2}{2D}. \tag{6}$$

Figure 3 shows some examples of calculated SPV transients ($n_0=2\times10^{10}$ cm^{-2}, $\varepsilon=10$). The value of λ_S was changed between 10 and 100 nm and the diffusion coefficients were varied between 10^{-3} and 10^{-8} cm^2/s. The peak time of the SPV transient is proportional to t_t (see the inset of Fig. 3, $t_{\text{peak}}\cong2.5t_t$). The SPV amplitude depends linearly on λ_S.

Considering the relation (1), the dielectric relaxation time definition and the Einstein relation $D=kT\mu/e$ a simple relation $t_t=\tau_M/2$ is obtained. The peak time of the SPV transient is proportional to τ_M ($t_{\text{peak}}\cong1.25\tau_M$). It is important to bring out that the dielectric relaxation time that is a bulk property can be obtained by SPV measurements that is a local technique, under the assumption (1).

From experimental point of view, the determination of t_{peak} may be complicated since t_{peak} may depend on additional processes as dielectric relaxation, local screening and diffusion to a certain distance including inhomogeneities. As an empirical value being sensitive practically only to diffusion over a distance of λ_S, the so-called logarithmic decay (τ_{LN}) time has been introduced. It is defined as the intercept of the slope in the inflection point of the SPV decay with the base line [Fig. 3(a)]. The value of τ_{LN} is two orders of magnitude larger than t_{peak}.

The log-log plot of the SPV transients [Fig. 3(b)] reflects nicely the increase and decay of the SPV transients by a power law. The power coefficients of 0.5 and −0.5 for the increasing and decaying parts of the SPV transients are obvious with respect to Eq. (5).

Photovoltage for anomalous diffusion

Very frequently, diffusion in condensed matter displays the behavior of anomalous diffusion due to disorder or inhomogeneities. Anomalous diffusion can be described with the fractional diffusion equations.[12] We consider the fractional diffusion equation concerning anomalous transport with a dispersion parameter α,

$$\frac{\partial}{\partial t}f(r,t)=C_{\alpha0}D_t^{1-\alpha}[\Delta f(r,t)], \tag{7}$$

where $f(r,t)$ is the concentration of the diffusive agent, C_α is the fractional diffusion constant (cm^2/s$^\alpha$ dimensions), Δ denotes the differential Laplace operator and ${}_0D_t^{1-\alpha}$ is the frac-

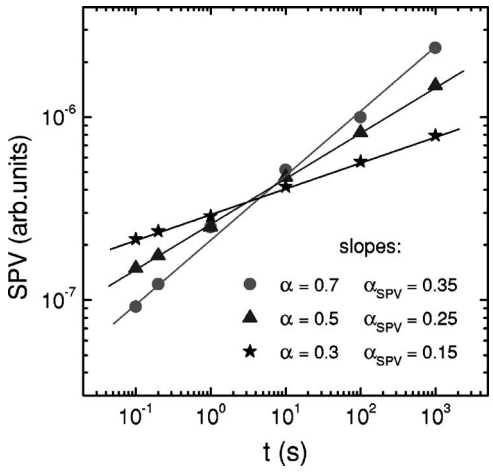

FIG. 4. SPV transients obtained by integration of the carrier distribution calculated by using anomalous diffusion with three power coefficients. See details in the text.

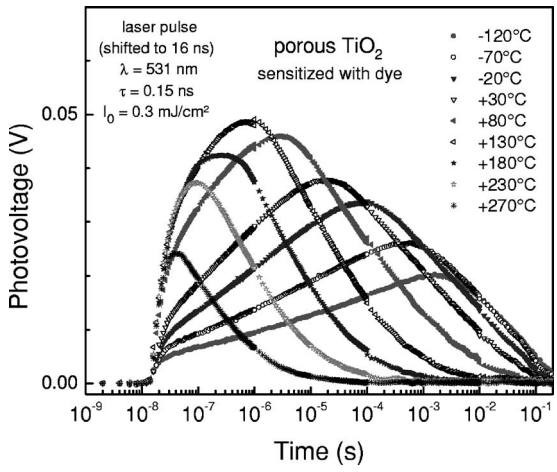

FIG. 5. SPV transients of nanoporous TiO_2 with adsorbed dye molecules at different temperatures. The laser pulse has been shifted to 16 ns.

tional Riemann-Liouville derivative operator of the order $0<\alpha<1$ and with lower limit $t=0$. Equation (7) is related[13,14] to the continuous time random walk (CTRW) formalism[15]. Equation (7) also describes the evolution of the total charge in the multiple trapping model.[16] The dispersion parameter is related to a distribution of trap states. In the case of a multiple trapping mechanism in an exponential distribution one has[17,18]

$$\alpha = \frac{T}{T_0}, \tag{8}$$

where T_0 is the parameter of the exponential distribution.

The mean square displacement for the anomalous diffusion model of Eq. (7) is $r^2 \propto C_\alpha t^\alpha$.[19] If the charge is conserved, and assuming the SPV is determined by the center of charge, it is obtained that the voltage changes with time as $U \propto r \propto t^{\alpha/2}$. For an exact solution of this problem we calculate in Appendix B the SPV using the solution of Eq. (7) in a semi-infinite space.[20] Figure 4 shows the increasing parts of SPV transients calculated for different dispersion parameters α of anomalous diffusion. It can be clearly seen that the SPV transients follow a power law with a power coefficient being half of the dispersion parameter of anomalous diffusion,

$$\mathrm{SPV}(t) \propto t^{\alpha/2}. \tag{9}$$

EXPERIMENT

For the experiment, nanoporous TiO_2 layers were prepared by screen printing of a paste containing anatase nanoparticles (diameter of the particles about 16 nm) and by subsequent firing in air at 450 °C for 30 min. Glass coated with conducting SnO_2:F served as a substrate for the nanoporous TiO_2 layers. Only the surface region of the nanoporous TiO_2 layers was sensitized with dye molecules (N3 -(Ru(dcbpyH$_2$)$_2$(NCS)$_2$)) by dipping in the 0.5 M dye solution for 10 s. Spectral surface photovoltage measurements showed the typical absorption behavior of the N3 dye molecules.

SPV transients were measured in the capacitor arrangement[21] with a thin mica layer used as a spacer. A 10 GΩ—load resistor, a high-impedance 500 MHz buffer (input resistance >100 GΩ, output resistance 50 Ω) and a 300 MHz—sampling oscilloscope were used for the transient measurements. The resolution time of the whole system was better than 2 ns. The RC time constant of the measuring circuit, i.e., sample with load resistor, was about 0.3 *s*. The SPV transients were excited with pulses of the second harmonic of a Nd:YAG laser (duration time 120 ps, wavelength 532 nm, excitation intensity at the sample $I_0=0.3$ mJ/cm^2). The repetition rate of the laser pulses was 1 Hz for all measurements.

The samples were placed in a homemade cryostate (pressure 10^{-6} mbar) allowing temperature dependent SPV measurements from the liquid nitrogen temperature up to about 300 °C. As found in previous experiments, N3 dye molecules adsorbed on TiO_2 are stable in high vacuum even at high temperatures.[11] In our opinion, this must be attributed to stabilization of the organic molecule by the strong binding to the TiO_2 via the four carboxylic groups.[22] Before cooling down the cryostate and starting the SPV measurements, the sample was conditioned inside the evacuated cryostate at 270 °C for 30 min. By this treatment, the influence of changing chemical reactions on the SPV experiments was avoided. The SPV measurements were performed at temperatures between −180 °C and 270 °C.

RESULTS AND DISCUSSION

Peak time and logarithmic decay time

Figure 5 shows SPV transients of nanoporous TiO_2 with adsorbed dye molecules at different temperatures. The laser pulse has been shifted to 16 ns for getting a better impression about the baseline and the time resolution (2 ns for the given experiments). At the relatively high excitation intensity I_0, the SPV signal rises within the resolution time of the system and increases further at longer times. The time at which the SPV transients reach the maximum increases strongly over

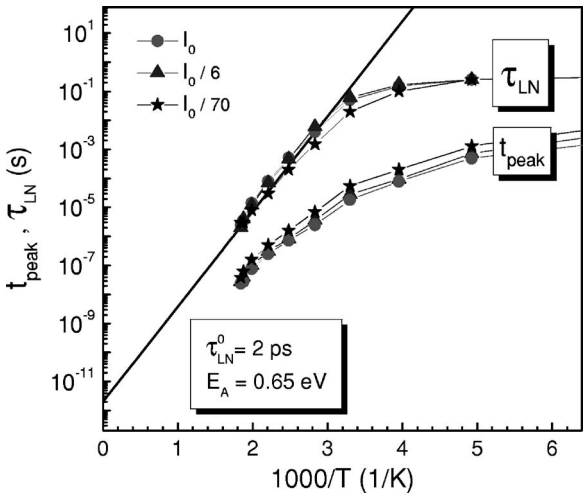

FIG. 6. Arrhenius plots of the peak and logarithmic decay times for three intensities of the laser pulse. The solid line gives the fit with E_A=0.65 eV and τ^0_{LN}=2 ps.

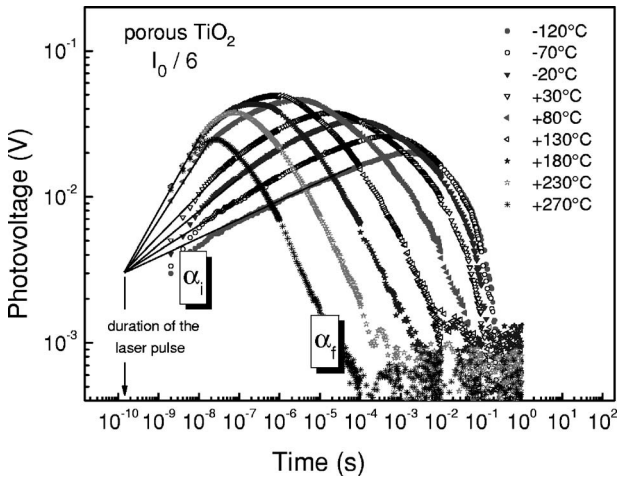

FIG. 7. Double logarithmic plots of SPV transients for different temperatures (intensities of the laser pulse 0.05 mJ/cm^2). The straight lines approximate the power laws to the duration time of the laser pulse.

several orders of magnitude with decreasing temperature. This time is of the order of the dielectric relaxation time[23] and its temperature dependence reflects the thermal activation of the conductivity.

The decays of the SPV transients follow a logarithmic law at low temperatures. As remark, logarithmic decays are well known from persistent photocurrents which are related to tunnel processes over a distribution of distances.[24] For this reason, a logarithmic dielectric relaxation instead of exponential as emphasized in Eq. (2) has been interpreted in terms of recombination limited by tunneling over short distances.[2,11] At higher temperatures, diffusion becomes dominant and pronounced tails develop at the longer times.

Figure 6 depicts the temperature dependencies of τ_{LN} and t_{peak} for three laser intensities. At low temperatures, τ_{LN} is constant since tunneling controls the relaxation of the SPV signal. At high temperatures, τ_{LN} is thermally activated due to thermal activation of electron diffusion in porous TiO_2. The obtained values of the activation energy (E_A) and of τ^0_{LN} are 0.65 eV and 2 ps, respectively. The observed activation energy is typical for the thermally activated conductivity in TiO_2.[25] For t_{peak}, the activation energy seems to change with temperature while E_A equals about 0.65 eV at the highest temperatures. As mentioned above, t_{peak} may be influenced by different processes which makes the interpretation of the temperature dependent activation energy rather complicated. At high temperatures, t_{peak} is shorter than τ_{LN} by two orders of magnitude, which is in excellent agreement with the simple model given by Eq. (5).

The value τ^0_{LN}=2 ps corresponds to an attempt rate of $\nu=5\times10^{11}$ s^{-1} which is typical for multiple trapping, for example, in amorphous Si.[26] Further, the value τ^0_{LN}=2 ps also reflects the shortest possible time for charge transfer of an electron back into a charged dye molecule. This is a much longer time than the electron transfer from the adsorbed dye molecule into the TiO_2 nanoparticles.[1]

Diffusion at different temperatures

Figure 7 shows the double logarithmic plots of SPV transients for different temperatures for a certain laser intensity. The SPV transients follow a power law at the shorter times of the increasing part. The power coefficients (α_i) depend strongly on temperature which is evidence for temperature dependent anomalous diffusion at short times. Further, the power law dependencies at the short times can be nicely approximated to a common intersection point at about 150 ps, i.e., the duration time of the laser pulse. This is a common property for all intensities of the laser pulse. Therefore, an initial distribution of excess electrons is formed within the duration of the laser pulse and anomalous diffusion of excess electrons can be observed immediately after switching off the laser pulse. The diffusion of excess electrons is controlled by hopping steps in a percolation network of available states. An elementary hopping step takes a time of the order of 2 ps which is much shorter than the duration time of the given laser pulse.

At very long times and higher temperatures, the decays of the SPV transients follow also a power law. In difference to the short times, the slopes at the long times are about α_f=0.5 independent of temperature. This means that normal diffusion controls the SPV relaxation at long times and higher temperatures. The obtained results demonstrate clearly that the SPV and its decay is controlled generally by diffusion over more than 10 orders of magnitude in time. There was no evidence for any exponential decay in all experiments. Therefore we can summarize the evolution as

$$\mathrm{SPV}(t) \propto t^{\alpha(T,W)/2} \quad (t \ll t_{\mathrm{peak}}),$$
$$\mathrm{SPV}(t) \propto t^{-1/2} \quad (t \gg t_{\mathrm{peak}}). \tag{10}$$

These observations indicate that the diffusion process is changing its character from anomalous diffusion at short times to normal diffusion at long decays. This is a general characteristic of carrier transport in disordered materials, as evidenced by the ac conductivity of many kinds of disordered solids, which changes from a constant dc value at low frequencies, to a frequency power law (related to anomalous

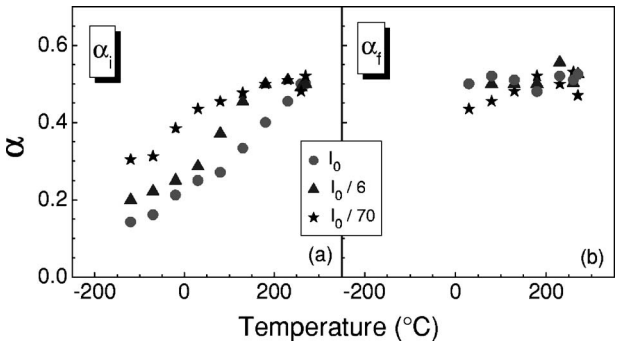

FIG. 8. Temperature dependence of the power coefficients of the increasing (a) and decaying (b) parts of the surface photovoltage transients for three intensities of the laser pulse.

diffusion) at high frequencies.[27] Recently, time-of-flight (TOF) experiments were performed under injection condition when the electron drift mobility is related to times much longer than the dielectric relaxation time. Under such condition, the electron drift mobility is nondispersive and controlled by the dark conductivity of porous TiO_2 (Ref. 8) and the thermal activation energy of the electron drift mobility is equal to that of the dark conductivity at high temperatures.[28] Therefore, with respect to the Einstein relation, electron diffusion is controlled as well by the dark conductivity of porous TiO_2 at long times and high temperatures.

Figure 8 depicts the values of α_i (a) and α_f (b) as a function of temperature for three values of laser intensity. The values of α_i increase with increasing temperature while they saturate at a value at about 0.5. For the highest laser intensity, the values of α_i start around 0.15 at the lowest temperatures. In contrast, this starting value of α_i increases to up to 0.3 (at −120 °C) with decreasing laser intensity. This means that the stationary concentration of excess electrons caused by the repetition rate of the laser pulse plays a crucial role for the dynamics of anomalous electron diffusion. This behavior is reasonable insofar as anomalous diffusion must be closely related to the stationary occupancy of electron traps. The anomalous diffusion exponent also changes with temperature. For example, in multiple trapping the exponent is linear with temperature, Eq. (8). However this result is exact only for a homogeneous concentration in a system with all the traps empty,[29] and these conditions are not realized in our measurement. We have found that Eq. (8) is only modestly obeyed by the results in Fig. 8.

Intensity dependent diffusion

Figure 9 shows SPV transients measured at room temperature for several laser intensities. The peak time shifts by about one order of magnitude towards shorter times with increasing laser intensity while the region of the maximum becomes nonsymmetric. The reason for this is probably some stationary excess charge remaining in the porous TiO_2 due to the repetition rate of the laser pulses of 1 Hz. Further, the SPV signal at the maximum does not scale linearly with the laser intensity.

At short times, the SPV transients follow nicely the power law while the power coefficients increase with decreasing

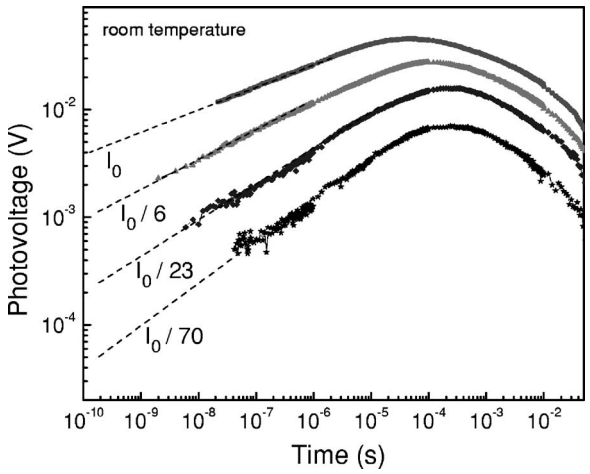

FIG. 9. SPV transients measured at room temperature for different intensities of the laser pulse.

laser intensity. The power law dependence of the SPV transients can be approximated to t_0=150 ps to get the initial SPV signal (PV (t_0)). The intensity dependence of (PV (t_0)) is shown in Fig. 10(a). The value of (PV (t_0)) depends linearly on the laser intensity over the whole range. This means that the distribution of the initial charge separation is independent of the laser intensity.

Figure 10(b) presents the dependence of the power coefficient α_i on the laser intensity (W) at room temperature. At low intensity, α_i is about 0.4. The value of α_i decreases with increasing W and saturates at about 0.2 for high laser intensities. This increasing dispersion with increasing W should be related to an increasing amount of excess charge carriers remaining stationary in the porous TiO_2 due to the repetition rate of the laser pulse. The detailed investigation of this behavior is beyond the scope of this work.

CONCLUSIONS

We observed normal and anomalous diffusion in porous TiO_2 for a wide temperature range by using transient surface

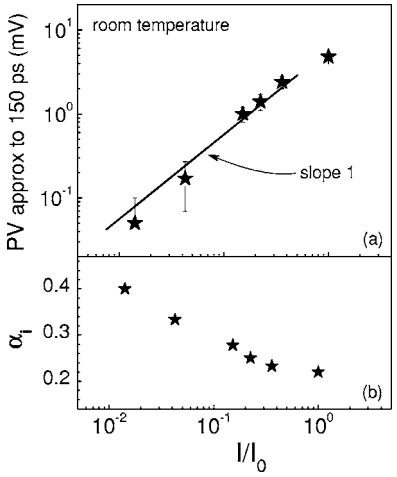

FIG. 10. Intensity dependence of the photovoltage approximated to the duration time of the laser pulse (a) and of the power coefficient for the increasing parts of the SPV transients.

photovoltage as a method for the investigation of transport. By doing so, one must take into account that the SPV is locally limited to the region where charge separation takes place, i.e., to a near surface layer with a thickness of the screening length. In future experiments, it will be interesting to investigate the role of local screening by the SPV technique for porous and mesoporous semiconductors in more detail.

The power-law approximation of the SPV to t_0 at different temperatures allows an extension of the information time about diffusion processes even to much shorter times than 100 ps if exciting the photovoltage with ultrashort laser pulses. Thus, the diffusion SPV opens new opportunities for getting information about spatial charge separation and diffusion down to very short times and for experimental conditions which are not applicable for conventional techniques such as time of flight.

ACKNOWLEDGMENTS

This work was supported by Ministerio de Educación y Ciencia of Spain under Contract No. MAT2004-05168 and by the DAAD (Acciones Integradas Projekt D/03/39275).

APPENDIX A

The solution of Eq. (4) with the delta function as initial distribution and with a blocking boundary condition at $x=0$ is a semi-Gaussian function

$$n(x,t) = \frac{n_i}{\sqrt{\pi Dt}} \exp\left(-\frac{x^2}{4Dt}\right). \tag{A1}$$

To obtain the SPV we employ Eq. (3). The first integration can be expressed as

$$\left.\frac{\partial U(t)}{\partial x}\right|_0^x = \frac{e}{\varepsilon\varepsilon_0}\int_0^x n(y,t)dy. \tag{A2}$$

Taking into account Eq. (A1),

$$-F(x,t) + F(0,t) = \frac{en_i}{\varepsilon\varepsilon_0} \operatorname{erf}\left(\frac{x}{2\sqrt{Dt}}\right), \tag{A3}$$

where F represents the electrical field and erf (z) is the error function defined as

$$\operatorname{erf}(z) = \frac{2}{\sqrt{\pi}}\int_0^z \exp(-s^2)ds. \tag{A4}$$

The electrical field at $x=\lambda_s$ is zero due to screening. Thus we obtain for the first integral

$$F(x,t) = \frac{en_i}{\varepsilon\varepsilon_0}\left[\operatorname{erf}\left(\frac{\lambda_s}{2\sqrt{Dt}}\right) - \operatorname{erf}\left(\frac{x}{2\sqrt{Dt}}\right)\right]. \tag{A5}$$

Considering

$$\int \operatorname{erf}(z) = z\operatorname{erf}(z) + \frac{\exp(-z)}{\sqrt{\pi}} \tag{A6}$$

we obtain the SPV as

$$\mathrm{SPV} = U(t) = \int_0^{\lambda_S} F(x,t)dx = \frac{2en_0}{\sqrt{\pi}\varepsilon\varepsilon_0}\sqrt{Dt}\left[1 - \exp\left(-\frac{\lambda_S^2}{4Dt}\right)\right]. \tag{5'}$$

APPENDIX B

To solve Eq. (7) the initial condition considered is

$$f(r,0) = f_0\delta(x), \tag{B1}$$

where $\delta(x)$ is the Dirac delta measure at the origin, $x=0$, and f_0 is the strength of the initial pulse concentration at the origin. If we consider electrons as the diffusive agent, $n=f$, the exact solution of Eq. (7) with the initial condition (B1) in the case of one-dimensional diffusion is[20]

$$n(x,t) = R(t)\sum_{k=1}^{\infty}[A(t,k)x^{2k} + B(t,k)x^{2k+1}], \tag{B2}$$

where $n_i=f_0$ and

$$R(t) = \frac{n_i}{\sqrt{4\pi C_\alpha t^\alpha}},$$

$$A(t,k) = \frac{(-1)^k\Gamma(1/2-k)}{(4C_\alpha t^\alpha)^k k!\Gamma[1-\alpha(1/2+k)]},$$

$$B(t,k) = \frac{(-1)^k\Gamma(-1/2-k)}{(4C_\alpha t^\alpha)^{k+1/2} k!\Gamma[1-\alpha(1+k)]}. \tag{B3}$$

Taking into account Eq. (B2) in Eq. (3), the SPV in the case of anomalous transport is

$$U(t) = \frac{eR(t)}{\varepsilon\varepsilon_0}\sum_{k=1}^{\infty}\left(\frac{A(t,k)}{(2k+1)(2k+2)}L^{2k+2} + \frac{B(t,k)}{(2k+2)(2k+3)}L^{2k+3}\right). \tag{B4}$$

Equation (B3) is valid if L is large enough so that $n(L,t) \approx 0$ holds, i.e., the sample is considered as a semi-infinite space. The numerical calculations were performed with cutting the series (B3) which introduced instabilities for large x. To exclude the instabilities in integration, the integration was performed between $x=0$ and x at which n leveled out to about 1%.

[1] K. Schwarzburg, R. Ernstdorfer, S. Felber, and F. Willig, Coord. Chem. Rev. **248**, 1259 (2004).
[2] V. Duzhko, V. Y. Timoshenko, F. Koch, and T. Dittrich, Phys. Rev. B **64**, 075204 (2001).
[3] M. Grätzel, Nature (London) **414**, 338 (2001).
[4] J. Bisquert, D. Cahen, S. Rühle, G. Hodes, and A. Zaban, J. Phys. Chem. B **108**, 8106 (2004).
[5] J. Nelson, S. A. Haque, D. R. Klug, and J. R. Durrant, Phys. Rev. B **63**, 205321 (2001).
[6] P. E. de Jongh and D. Vanmaekelbergh, Phys. Rev. Lett. **77**, 3427 (1996).
[7] L. Kronik and Y. Shapira, Surf. Sci. Rep. **37**, 1 (1999).
[8] V. Kytin, T. Dittrich, J. Bisquert, E. A. Lebedev, and F. Koch, Phys. Rev. B **68**, 195308 (2003).
[9] V. Duzhko, thesis, 2003.
[10] S. M. Sze, *Physics of Semiconductor Devices*, 2nd ed. (Wiley, New York, 1981).
[11] I. Mora-Seró, T. Dittrich, A. Belaidi, G. Garcia-Belmonte, and J. Bisquert, J. Phys. Chem. B **109**, 8035 (2005).
[12] R. Metzler and J. Klafter, Phys. Rep. **339**, 1 (2000).
[13] R. Hilfer, J. Phys. Chem. B **104**, 3914 (2000).
[14] R. Hilfer, in *Anomalous Diffusion-From Basics to Applications*, edited by R. Kutner, A. Pekalski, and K. Sznaij-Weron (Springer, Berlin, 1999), p. 77.
[15] H. Scheer and E. W. Montroll, Phys. Rev. B **12**, 2455 (1975).
[16] J. Bisquert, Phys. Rev. Lett. **91**, 010602 (2003).
[17] J. Orenstein and M. Kastner, Phys. Rev. Lett. **46**, 1421 (1981).
[18] T. Tiedje and A. Rose, Solid State Commun. **37**, 49 (1981).
[19] R. Metzler, E. Barkai, and J. Klafter, Phys. Rev. Lett. **82**, 3563 (1999).
[20] Y. E. Ryabov, Phys. Rev. E **68**, 030102(R) (2003).
[21] E. O. Johnson, J. Appl. Phys. **28**, 1349 (1957).
[22] H. Rensmo, K. Westermark, S. Södergren, O. Kohle, P. Persson, S. Lunell, and H. Siegbahn, J. Chem. Phys. **111**, 2744 (1999).
[23] V. Duzhko, F. Koch, and T. Dittrich, J. Appl. Phys. **91**, 9432 (2001).
[24] H. J. Queisser and D. E. Theodorou, Phys. Rev. B **33**, 4027 (1986).
[25] T. Dittrich, J. Weidmann, F. Koch, I. Uhlendorf, and I. Lauermann, Appl. Phys. Lett. **75**, 3980 (1999).
[26] T. Tiedje, J. M. Cebulka, D. L. Morel, and B. Abeles, Phys. Rev. Lett. **46**, 1425 (1981).
[27] J. C. Dyre and T. B. Schroder, Rev. Mod. Phys. **72**, 873 (2000).
[28] T. Dittrich, J. Weidmann, V. Y. Timoshenko, A. A. Petrov, F. Koch, M. G. Lisachenko, and E. Lebedev, Mater. Sci. Eng., B **69-70**, 489 (2000).
[29] J. Bisquert, Phys. Rev. E **72**, 011109 (2005).